

A Numerical Strategy to Design Maneuverable Micro-Biomedical Swimming Robots Based on Biomimetic Flagellar Propulsion

Arash Taheri, Meysam Mohammadi-Amin, Seyed Hossein Moosavy

Abstract—Medical applications are among the most impactful areas of microrobotics. The ultimate goal of medical microrobots is to reach currently inaccessible areas of the human body and carry out a host of complex operations such as minimally invasive surgery (MIS), highly localized drug delivery, and screening for diseases at their very early stages. Miniature, safe and efficient propulsion systems hold the key to maturing this technology but they pose significant challenges. A new type of propulsion developed recently, uses multi-flagella architecture inspired by the motility mechanism of prokaryotic microorganisms. There is a lack of efficient methods for designing this type of propulsion system. The goal of this paper is to overcome the lack and this way, a numerical strategy is proposed to design multi-flagella propulsion systems. The strategy is based on the implementation of the regularized stokeslet and rotlet theory, RFT theory and new approach of “local corrected velocity”. The effects of shape parameters and angular velocities of each flagellum on overall flow field and on the robot net forces and moments are considered. Then a multi-layer perceptron artificial neural network is designed and employed to adjust the angular velocities of the motors for propulsion control. The proposed method applied successfully on a sample configuration and useful demonstrative results is obtained.

Keywords—Artificial Neural Network, Biomimetic Microrobots, Flagellar Propulsion, Swimming Robots.

I. INTRODUCTION

MINIATURE swimming robots could be greatly beneficial for screening and treatment of many diseases.

Due to their small size, micro swimming robots operate in very small Reynolds (Re) number. A low Reynolds number infers that inertial forces are less significant or even negligible compared to viscous forces. Therefore, microscale swimmers in general experience drastically different hydro-dynamics compared to conventional swimming robots. Thus, propulsion mechanisms generally used in macroscale swimming robots may fail in micro scales. This problem motivates researchers to develop new concepts and design efficient systems for the propulsion of swimming microrobots. Following on, some of the important related works are reviewed and discussed.

A. Taheri is with the Aerospace Faculty, Sharif University of Technology, Tehran, Iran (e-mail: taheri.cfd@gmail.com).

M. Mohammadi-Amin is with the Department of Mechanical Engineering, Tarbiat Modares University, Tehran, Iran, P.O. Box 14115-385 (Phone: +989122515702; e-mail: mohammadi_amin@modares.ac.ir).

S.H. Moosavi is with the Department of Mechanical Engineering, Tarbiat Modares University, Tehran, Iran (e-mail: s.hossein.moosavy@gmail.com).

There are few biomimetic swimming robot, mostly fin-driven, developed [1]-[4]. Since fish-like biomimetic robots rely on inertial forces for propulsion, miniaturization will make them ineffective [1]. Another design was introduced by Honda, Arai and Ishiyama [4]. In this method an external magnetic field is used to rotate a small ferromagnetic screw in liquid. The advantages of this machine are that it does not require any power source or controller on the machine and it is not tethered which makes it very attractive for medical purposes. It has been demonstrated that this spiral type machine can swim in liquids of various viscosities in a broad range of Re numbers. However, speed limitation is the main disadvantage of this machine. For the frequency higher than the frequency which corresponds to the maximum acquirable speed, the rotation of the machine could not synchronize to the rotational frequency of the external field and the velocity decreased. Besides the speed limitation issue, there are other issues associated with the usage of a magnetic field: (1) Patients with pacemakers, metal implants and bullet wounds can not be subjected to magnetic fields. Magnetic force can pull on these objects, cutting and compressing healthy tissue. (2) Considering the low speed of the robot, the patient may be required to stay in the magnetic field for longer than the time allowed by FDA regulations. (3) Gradient fields can produce eddy currents in the patient and cause heating. This is not usually a concern in Magnetic Resonance Imaging (MRI), but it might become an issue if the robot is moving inside the body. In 2006 Behkam and Sitti [5] proposed a novel safe, miniature and energy efficient propulsion system potentially used for all patients with no restriction. Also, the proposed method does not subject the patients to the discomfort of staying in magnetic field for an extended period of time. Their proposed biomimetic propulsion concept is inspired by the peritrichous flagellation used by bacteria such as E. Coli, depicted in Fig. 1. The flagella of these cells are randomly distributed over the cell surface and each flagellar motor rotates independently of the others. Hydrodynamic interactions among flagella cause them to coordinate, coalescing and bundling behind the cell during swimming [6]. The flagellum is a propulsive organelle that includes a reversible rotary motor embedded in the cell wall, and a filament that extends into the external medium [7]. The filament is a long (~10 μm), thin (~20nm) helix (2.5 μm pitch, 0.5 μm diameter) that turns at speed of ~100 Hz. This

propulsion system can perform effectively even at very small scale and low Re numbers.

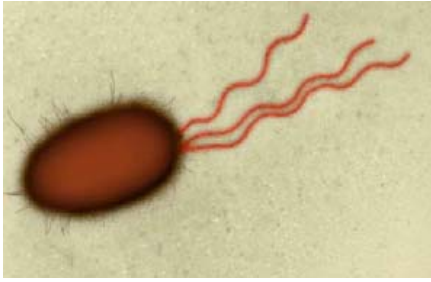


Fig. 1 Transmission electron microscopy (TEM) image of E. Coli

On the other hand, the Behkam and sitti's model is a theoretical approach and is only applicable to single flagellum architecture [5]. For multi-flagella concept that is presented and examined by Taheri and Mohammadi-Amin [8], the numerical approach should be used. This propulsion method is suitable for the swimming robots which are intended to swim in low velocity biofluids. Potential target regions to use these robots include eyeball cavity, cerebrospinal fluid and the urinary system. In this paper, we present a novel concept and numerical strategy to design multi-flagella architecture of swimming robots. This architecture has some important advantages with respect to single flagellum architecture: more propulsion, enhancement of maneuverability, better capability to optimum design (more design parameters) and last but not least, it's a natural rule!

II. LOW REYNOLDS NUMBER FLOW MODELING

Reynolds number is defined as $\rho vl/\mu$, where ρ and μ are density and dynamic viscosity of the fluid, respectively, v is the flow velocity and l is the characteristic dimension of the object. Reynolds number is defined as the ratio of inertia forces to viscous forces and characterizes the fluid flow. For the micro scale objects moving in water, due to the size of the object and fluid properties, $Re \ll 1$, that means viscous effects are dominant and inertial forces are insignificant. For this type of flow Navier-Stokes equations reduces. So fluid dynamics in problems of microorganism motion and microrobots, where length and velocity scales are very small, is well-modeled by the Stokes equations for incompressible flows,

$$0 = -\nabla P + \mu \Delta U + f \quad , \quad 0 = \nabla \cdot U \quad (1)$$

III. NUMERICAL STRATEGY

In this research, the multi-flagella propulsion system with separate motor for each flagellum (Fig.2) is investigated using regularized 3D stokeslet and rotlet theory. The rigid (not flexible) multi-flagella dynamic is modeled by forces applied on the flagella points and by a torque at the base of each using regularized stokeslet and rotlet theory [6], [9].

A. Solution of Stokes Equations

The fluid velocity field due to the forces is described by regularized stokeslets and the velocity due to the torques by the associated regularized rotlets. In the typical stokeslet & rotlet theory, singularities in the velocity expression are due to the assumption of having point-forces and point-torques. However, by regularized approach, the singularities can be eliminated through the systematic regularization of the flows described above by considering forces and torques that are applied not at single points but within small spheres centered at those points. In this way, the forces and torques are highly concentrated but are spread over a small neighborhood of the application points. The regularized 3D stokeslet and rotlet solution is given by [6],

$$U = \sum_{i=1}^{N_r} U_{\delta,r}(x; y_i, L_i) + \sum_{j=1}^{N_s} U_{\delta,s}(x; z_j, f_j) \quad (2)$$

where N_r is the number of rotlets of strengths L_i located at y_i and N_s is the number of stokeslets of strengths f_j located at z_j and we have,

$$U_{\delta,r}(x; y_i, L_i) = \frac{(2r^2 + 5\delta^2)}{16\pi(r^2 + \delta^2)^{5/2}} [L_i \times (x - y_i)] \quad (3)$$

$$U_{\delta,s}(x; z_j, f_j) = \frac{f_j(r^2 + 2\delta^2)}{8\pi(r^2 + \delta^2)^{3/2}} + \frac{[f_j \cdot (x - z_j)](x - z_j)}{8\pi(r^2 + \delta^2)^{3/2}} \quad (4)$$

Notice that as δ approaches zero, we recover the original stokeslet/rotlet expression. This formula expresses analytical solutions to a regularized version of the Stokes equations in which the forces and torques are not applied at single points, but are distributed over a small neighborhood of the application point [6]. This closed form solutions give us a velocity field that can be used to track moving particles in the fluid. In our numerical approach, for flow field simulation by stokeslet and rotlet, all flagella are divided to finite number of nodes and forces on these nodes are estimated by Resistance Force Theory and new approach of "local corrected velocity" which uses the velocity field of previous iteration to calculate the local normal and tangential velocities when the helical structure rotates. This way considers the effects of neighbor flagella in calculations [8]. The geometrical parameters of a flagellum are shown in the figure (3).

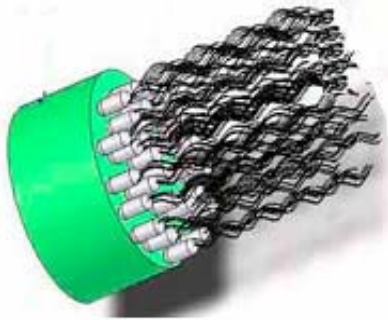


Fig. 2 A typical multi-flagella architecture for swimming robot in micro-scale (N=50 flagella)

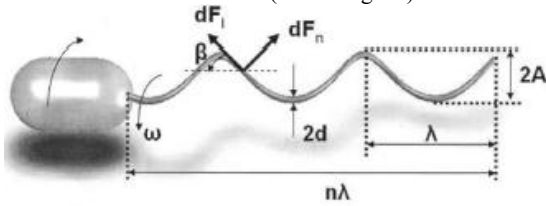


Fig. 3 Schematic of the microscale swimming robot with helical wave propulsion (single flagellum)

B. RFT Theory

Hancock developed very useful relationships for calculating the normal and tangential coefficients of viscous resistance acting on the surface of a long thin cylindrical filament moving through a viscous fluid. This is known as resistive force theory (RFT). The tangential and normal forces acting on a cylindrical element of length ΔS according to RFT (coupled with local corrected velocity approach) are in the following form,

$$\begin{aligned} \Delta F_n &= -C_{n,helix} V_n^{old} \Delta S \\ \Delta F_t &= -C_{t,helix} V_t^{old} \Delta S \end{aligned} \quad (5)$$

where V_n and V_t are the normal and tangential velocities at the flagellum node at previous time respectively, and $C_{n,helix}$ and $C_{t,helix}$ are the corresponding coefficients of resistance driven empirically by Johnson & Brokaw [10] for a flagellum with both free ends,

$$C_{n,helix} = \frac{4\pi\mu}{\ln\left(\frac{2\lambda_{helix}}{d_{helix}}\right) + \frac{1}{2}} \quad (6)$$

$$C_{t,helix} = \frac{2\pi\mu}{\ln\left(\frac{2\lambda_{helix}}{d_{helix}}\right) - \frac{1}{2}} \quad (7)$$

After forces calculation at all flagella nodes in each time step, we simulate the overall flow field around the robot. By considering a cylindrical control volume just around the propulsion system and applying the Newton's second law to

it, we calculate the net propulsion (forces & moments) produced by the multi-flagella system. By this approach, we investigate the effects of flagella shape parameters such as flagella thickness and angular velocities (with its direction) of each flagellum on overall flow field around the robot and on the robot net forces and net moments. As it is clear, a designer has more parameters to reach optimum design for a specific mission in this kind of multi-flagella microrobots.

C. ANN for Propulsion Control

For trajectory control of the swimming robot, firstly, designer should know the relation between the forces and moments and angular velocities of the flagella to adjust the rotation rate of the motors for a given required loading ($f_x, f_y, f_z, M_x, M_y, M_z$). By our numerical strategy, we can set the rotation rates of flagella and calculate the forces and moments on the robot but now we have an inverse problem. In general, the relation between these loading and angular velocities is complex and fully nonlinear in nature, so we should treat a careful trend.

In terms of new methodologies for multi-dimensional estimation, neural networks are promising technology because of their ability to be trained and used for investigation of systems that involve nonlinear dynamics. Because of this proven capacity, neural networks have been applied in system identification. An artificial neural network (ANN) is a massively parallel distributed processor made up of interconnected processing units. The fundamental information processing unit is called as neuron or node, which is the mathematical abstraction of the neuron in the biological science [11]. One popular and successfully applied ANN model is the multi-layer perceptron (MLP). The MLP has a multilayer feed-forward configuration, and it is trained in a supervised (target-oriented) manner with the highly popular error back-propagation learning algorithm. Typically the MLP has input, hidden, and output layers. Note that a synaptic weight is associated with each connection. Error back-propagation learning consists of two passes through the network on a layer-by-layer basis: a forward pass and a backward pass. During the forward pass the synaptic weights of the network are all fixed.

In this research, we have designed a multi-layer perceptron neural network (MLPR) with one hidden layer. For example, for a robot with N=3 flagella the MLPR has the 6-50-3 architecture. This ANN is employed to estimate the angular velocities of the motors for a given ($f_x, f_y, f_z, M_x, M_y, M_z$) (fig.4). For ANN training, the results of the computational code (based on stokeslet & rotlet theory) for different angular velocity combinations include positive and negative directions of rotation are used. After training, the ANN learns the relation between inputs and outputs and is used to adjust flagella angular velocities.

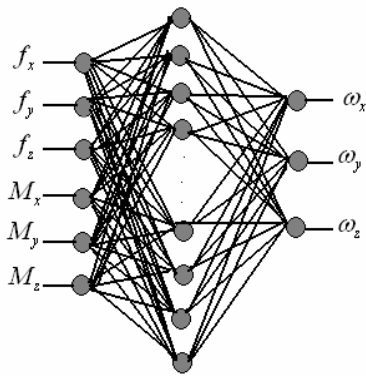


Fig. 4 Schematic of the ANN Architecture (6-50-3) for propulsion control, N=3 flagella

To have optimum accuracy and computational cost, it is necessary to examine different learning rates in neural network training. Figure 5 shows the convergence history of the problem for the best results base on solution accuracy and computational effort which are obtained for learning rate equals to 0.005. As it is clear, for greater learning rate values, we have less accuracy but more convergence rate. As is shown in the figure 6, by selection of the learning rate greater than 0.006, one can see more serious oscillations in convergence history and faster error increase. The activation functions in ANN should be continuous, in this research the activation functions in hidden and output layers are the tangent hyperbolic and linear function respectively. The ANN has been tested for some test cases and results indicate good agreement between the ANN predictions and the computational code. For instance, the below table shows a comparison between ANN predictions for the case with given ($f_x, f_y, f_z, M_x, M_y, M_z$) and the exact values with the same loading (generated by code). So the trained ANN can be used to adjust the angular velocities of the flagella of the robot to achieve the required forces/moments for tracking a trajectory.

TABLE I
 ANN RESULT FOR AN EXAMPLE CASE

Angular velocities	ω_1 (Hz)	ω_2 (Hz)	ω_3 (Hz)
Computational code	-800	-800	+800
ANN results	-801.13	-799.83	799.89

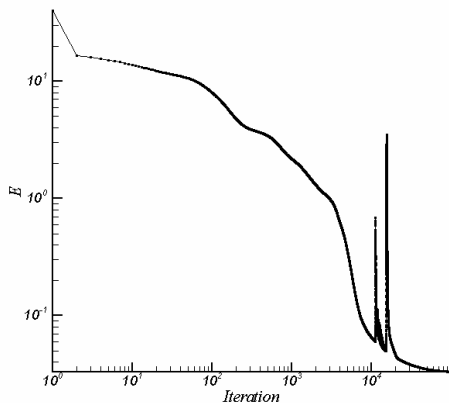


Fig. 5 Learning history diagram for the best learning rate = 0.005 for N=3 flagella

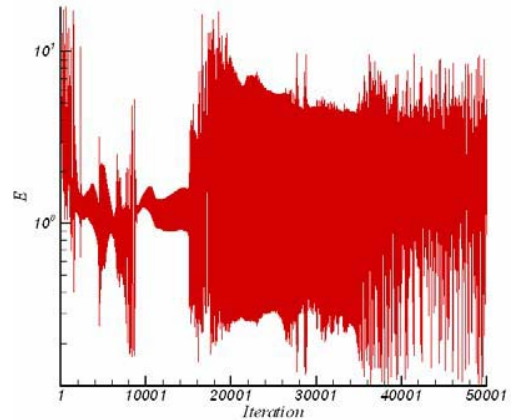


Fig. 6 Learning history diagram in unstable region for learning rate = 0.008 for N = 3 flagella

IV. RESULTS

The figure 7 indicates a comparison between the results of our numerical approach and behkam's theoretical model for the single flagellum case that are in good agreement and validates our approach. Figures 8 and 9 shows the flow field produced by three-flagella propulsion system (two clockwise and one counterclockwise) with rotation rates of 800 Hz.

As you see the axial velocity in this manner produces the effective thrust force and moments for the microrobot to change its heading but single flagellum microrobot is weak in this action. This fact is compatible with the experimental observations conducted using a small three-flagellar swimming robot (fig. 10). So as it's clear, the multi-flagellar based robots are more maneuverable and they just need an efficient control system such as an ANN-based electrical chip.

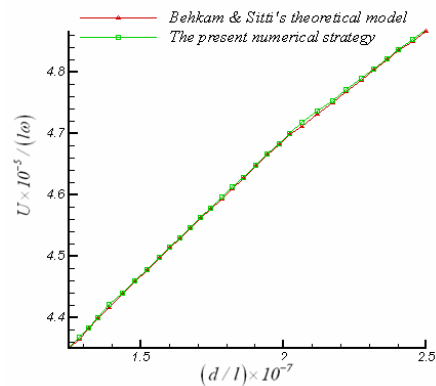


Fig. 7 Comparison between the numerical and theoretical results for robot velocity for single flagellum case

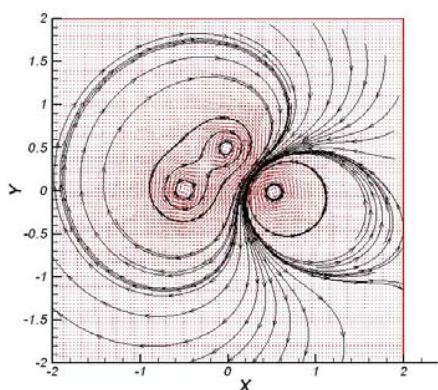


Fig. 8 Computed flow field (view from behind the robot)

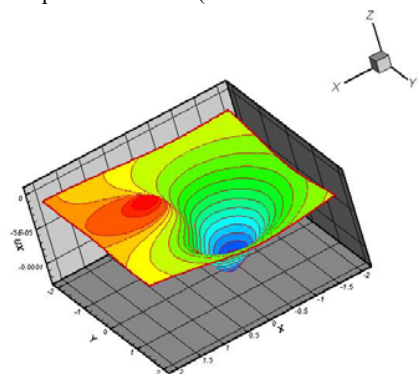


Fig. 9 Axial velocity viewed from behind the robot for N=3 flagella



Fig. 10 testing model for multi-flagella propulsion concept

V. CONCLUSION

In this paper, a numerical strategy is proposed to design multi-flagella propulsion systems. The strategy is based on the implementation of the regularized stokeslet and rotlet theory, RFT theory and new approach of “local corrected velocity”. Then a multi-layer perceptron artificial neural network is designed and employed to adjust the angular velocities of the motors for propulsion control. The proposed method applied successfully on a sample configuration with three flagella. Microrobots with this kind of propulsion system can be used in the human body regions with low flow inertia like eyeball cavity, cerebrospinal fluid and urinary system.

REFERENCES

[1] T. Fukuda, A. Kawamoto, F. Arai, and H. Matsuura, “Mechanism and swimming experiment of micro mobile robot in water,” *Proc. of IEEE Int'l Workshop on Micro Electro Mechanical Systems (MEMS'94)*, pp.273-278, 1994.

[2] S. Guo, Y. Hasegawa, T. Fukuda, and K. Asaka, “Fish –Like underwater microrobot with multi DOF,” *Proc. of 200 International Symposium on Micromechatronics and Human Science*, pp. 63-68, 2001.

[3] J. Jung, B. Kim, Y. Tak and J. Park, “Undulatory tadpole robot (TadRob) using ionic polymer metal composite (IMPC) actuator,” *Proc. of the 2003 IEEE/RSJ International Conference on Intelligent Robots and Systems*, pp. 2133-2138, 2003.

[4] T. Honda, K. Arai and K. Ishiyama, “Effect of micro machine shape on swimming properties of the spiral-type magnetic micro-machine,” *IEEE Transaction on Magnetics*, vol. 35, pp. 3688-3690, 1999.

[5] B. Behkam, M. Sitti, “Design Methodology for biomimetic propulsion of miniature Swimming Robots,” *J. Dynamic Systems Measurement and Control*, Vol. 128, pp.136-43, 2006.

[6] H. Flores, E. Lobaton, S. Mendez-Diez, S. Tlupavova and R. Cortez, “A study of bacterial flagellar bundling,” *Bulletin of Mathematical Biology*, vol. 67, pp.137-168, 2005.

[7] H. Berg, “The Rotary Motor of Bacterial Flagella,” *Annual Review of Biochemistry*, Vol.72, pp. 19-54, 2003.

[8] A. Taheri. M. Mohammadi-Amin, “Towards a multi-flagella architecture for E.Coli Inspired swimming microrobot propulsion,” *Proc. 8th World Congress on computational mechanics & 5th European Congress on Computational Methods in Applied Sciences and Engineering*, Venice, Italy, 30 June-4 July, 2008.

[9] R. Cortez, “The method of regularized stokeslet,” *SIAM J. of Sci. Computing*, Vol. 23, pp.1204-1225, 2001.

[10] R. E. Johnson, and C. J. Brokaw, “Flagellar hydrodynamics: A comparison between resistive-force theory and slender-body theory,” *Biophys. J.*, Vol.125, pp.113-127, 1979.

[11] M. B. Menhaj, *Computational Intelligence: Fundamental of Neural Networks*, Amirkabir University of Technology Publication, Tehran, 2000.

[12] Y. Zhang, Q. Wang, P. Zhang, X. Wang, and T. Mei, “Dynamic analysis and experiment of a 3mm swimming microrobot,” *Proc. of the 2004 IEEE/RSJ International Conference on Intelligent Robots and Systems*, pp. 1746-1750, 2004.